



## A new low gain avalanche diode concept: the double-LGAD

F. Carnesecchi<sup>1,a</sup>, S. Strazzi<sup>2,5,b</sup>, A. Alici<sup>2,5</sup>, R. Arcidiacono<sup>3,4</sup>, N. Cartiglia<sup>3</sup>, D. Cavazza<sup>5</sup>, S. Durando<sup>7</sup>, M. Ferrero<sup>3</sup>, A. Margotti<sup>5</sup>, L. Menzio<sup>3,6</sup>, R. Nania<sup>5</sup>, B. Sabiu<sup>2,5</sup>, G. Scioli<sup>2,5</sup>, F. Siviero<sup>3</sup>, V. Sola<sup>3,6</sup>, G. Vignola<sup>5</sup>

<sup>1</sup> CERN, Geneva, Switzerland

<sup>2</sup> Dipartimento Fisica e Astronomia, Università di Bologna, Bologna, Italy

<sup>3</sup> INFN, Torino, Italy

<sup>4</sup> Università del Piemonte Orientale, Novara, Italy

<sup>5</sup> INFN, Bologna, Italy

<sup>6</sup> Università degli Studi di Torino, Torino, Italy

<sup>7</sup> Dipartimento di elettronica e telecomunicazioni, Politecnico di Torino, Torino, Italy

Received: 29 July 2023 / Accepted: 22 October 2023

© The Author(s) 2023

**Abstract** This paper describes the new concept of the double LGAD (low-gain avalanche diodes). The goal was to increase the charge at the input of the electronics, keeping a time resolution equal to or better than a standard (single) LGAD; this has been realized by adding the charges of two coupled LGADs while still using a single front-end electronics. The study here reported has been done starting from single LGAD with a thickness of 25  $\mu\text{m}$ , 35  $\mu\text{m}$  and 50  $\mu\text{m}$ .

### 1 Introduction

Low-gain avalanche diodes (LGADs) [1], also known as ultra-fast silicon detectors (UFSDs) [2] when optimized for timing, are  $n$ -on- $p$  diodes with an additional highly doped  $p^+$ -type layer (gain layer) underneath the  $n$ -contact, which is responsible for the charge multiplication mechanism (in reverse bias regime). It has been proven that LGADs with a thickness of 35  $\mu\text{m}$  combined with a gain  $G \sim 30$  can provide a time resolution around 22 ps [3].

Thanks to the excellent timing performance, this technology is already envisioned or proposed for several detector upgrades and applications [4–6].

It has already been demonstrated that the time resolution of LGADs improves with thinner designs. Nevertheless, a thinner design also implies a smaller charge at the input of the amplifier which, because of the worse S/N, might worsen the performance of the amplifier and/or its power consumption. This need gave rise to the idea of the double LGAD.

### 2 The double LGAD

The concept of the double LGAD (d-LGAD) is inspired by the multigap resistive plate chambers (MRPC) [7]. Essentially, the idea is to sum up the signal taken from a double layer of LGADs, still using a unique front-end amplifier.

As a first step, the signals from two different LGADs have been summed using a specific PCB design (more details in Sect. 3.2) and the output has been sent to a single and common amplifier. In Fig. 1, a schematic of a d-LGAD is reported. This is currently just a proof of concept, but the natural next step would be a better integration of such a concept either in the board containing the electronics or in the detector itself (in a truly d-LGAD or e.g. using through-silicon via (TSV) technique). The possibility to implement the d-LGAD in the detector could allow an easy extension to multi-channel LGADs, although an ad hoc study and simulation in collaboration with the producer would be required.

In the proposed scheme, given by the sum of two LGADs each with a certain thickness  $t$ , the charge of the d-LGAD is expected to be double if compared with a single LGAD of same thickness  $t$ . The time resolution of such a d-LGAD is expected to be largely better than that of an equivalent single LGAD of thickness  $2t$  [2]. Similar to MRPC [8], the time resolution of a d-LGAD is foreseen to improve also with respect to a single LGAD of thickness  $t$ ; however, due to different signal amplitudes in the two d-LGADs, this improvement is less of what expected from simple scaling (i.e. a factor of  $\sqrt{2}$ ). As stated in [8], the time resolution will be dominated by the d-LGAD with the largest signal. The largest signal gives the earliest threshold crossing time, so the timing of the d-LGAD

<sup>a</sup> e-mail: francesca.carnesecchi@cern.ch (corresponding author)

<sup>b</sup> e-mail: sofia.strazzi2@unibo.it (corresponding author)

**Fig. 1** Schematic of the single-LGAD (standard) and double-LGAD concept

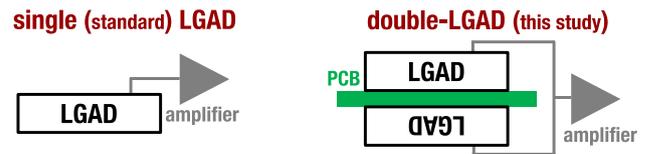


**Table 1** Characteristics of the front (F) and back (B) LGADs of each couple under test

	$A$ (mm <sup>2</sup> )	$T$ (μm)	$V_{bd}$ (V)	$V_{applied}$ (V)	Gain
FBK25-F	1 × 1	25	132 ± 1	80–120	11–24
FBK25-B	1 × 1	25	124 ± 1	80–120	12–43
FBK35-F	1 × 1	35	266.5 ± 0.5	180–240	9–17
FBK35-B	1 × 1	35	268 ± 1	190–240	11–27
HPK50-F	1.3 × 1.3	50	224.6 ± 0.2	170–220	24–63
HPK50-B	1.3 × 1.3	50	237.4 ± 0.2	170–220	25–64

is approximately given by the earliest LGAD. In other words, in d-LGAD, the LGAD with the largest signal always dominates the time resolution.

### 3 Experimental set-up

#### 3.1 Detectors

The tested LGADs came from two manufacturers, namely Hamamatsu Photonics K.K. (HPK, Japan) and Fondazione Bruno Kessler (FBK, Italy), and have a different area ( $A$ ). The sensors from HPK have a nominal thickness ( $T$ )<sup>1</sup> of 50 μm, appertaining to a very uniform wafer (if compared to FBK sensors, as evident from the gain reported in Table 1 for same thickness sensors). The FBK LGADs<sup>2</sup> have a nominal thickness of 25 μm and 35 μm, respectively. More details about the FBK LGADs characteristics and performances can be found in [3].

All the tested detectors have been previously completely characterized at the INFN Bologna laboratories. The methods to measure the breakdown voltage ( $V_{bd}$ ) gain are explained in [3]. The main characteristics of the sensors are reported in Table 1.

#### 3.2 Beam test set-up and electronics

The time resolution of the UFSDs has been studied at the T10 beamline at PS-CERN in July and November 2022. The beam was mainly composed of protons and pions with a momentum of +10 GeV/c. For each data acquisition, up to four carrier boards mounted on micro-mover stages were aligned to the beam in a telescope frame at a relative distance of 24 cm, and the whole set-up was enclosed in a dark environment box at room temperature.

All the LGADs tested have been mounted on a board V1.4-SCIPP-08/18, containing a wide-bandwidth (2 GHz) and low-noise inverting amplifier with a measured amplification of factor 6. The board has been modified in order to place one LGAD on each side of the board and, thanks to a via in the printed circuit board (PCB) itself, connect the output of the two LGADs together and send the signal to the amplifier described above, realizing a first prototype of d-LGAD. The output of the board was followed by a second amplification stage, with a gain factor of around 13 and 14, respectively, for the HPK50 and FBK sensors.<sup>3</sup>

Up to four amplified signals were sent to a LeCroy WaveRunner 9404 M-MS oscilloscope,<sup>4</sup> with 20 Gs/s sampling rate, 4 GHz of analogue bandwidth and 8-bit vertical resolution. The contribution of the oscilloscope time resolution to the measured one was negligible.

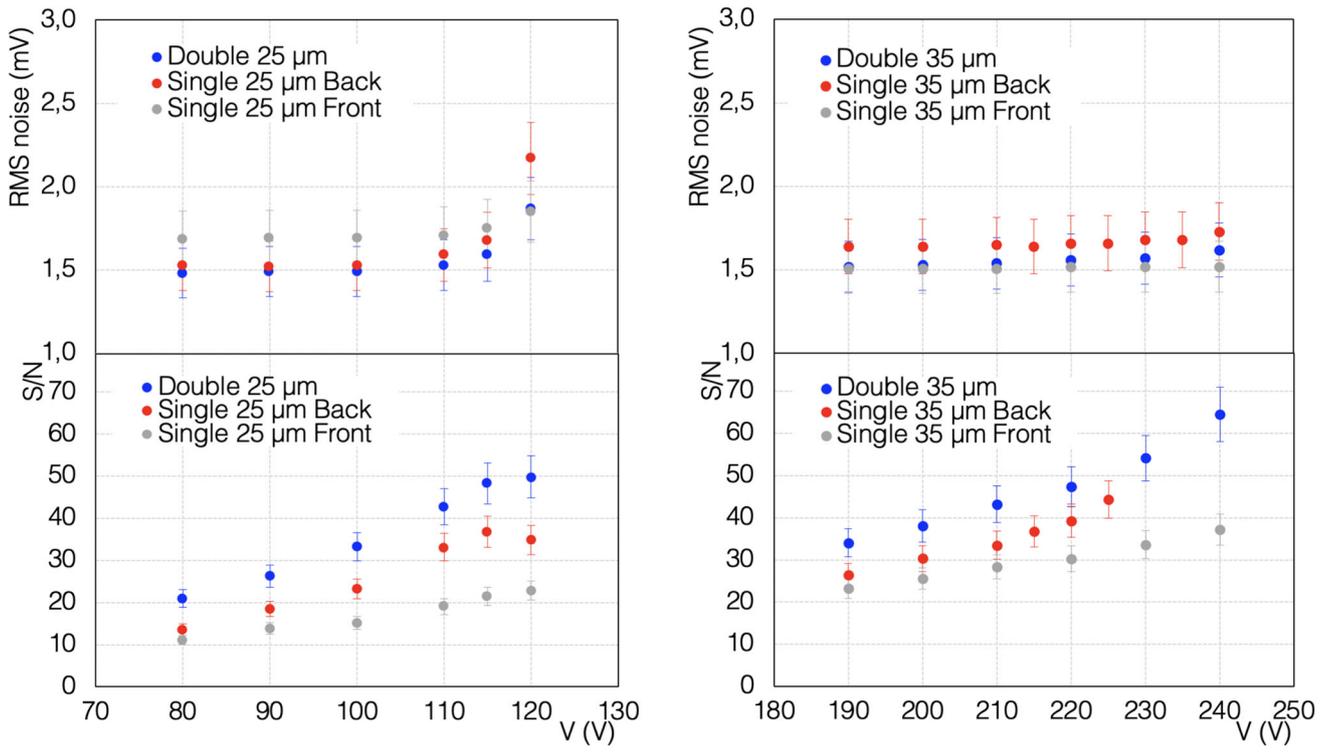
For the trigger of the data acquisition, a threshold has been set for each channel and the coincidence of the four sensors has been used.

<sup>1</sup> Usually, the active thickness is around 2–3 μm less than the nominal.

<sup>2</sup> This UFSD production is called EXFLU0 [9].

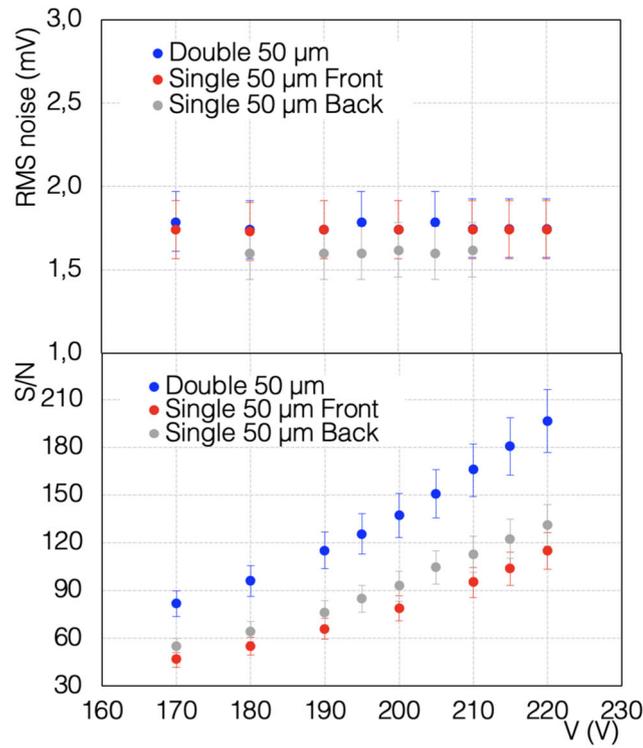
<sup>3</sup> The second amplifier used for the HPK50 and that used for the FBK sensors were the minicircuit LEE39+ (LEE39+datasheet) and Gali52+ (GALI52+datasheet), respectively.

<sup>4</sup> Lecroy WaveRunner datasheet.



(a)

(b)



(c)

**Fig. 2** RMS of the noise and S/N ratio for all the tested LGADs 25 (a), 35 (b) and 50 (c) micrometer

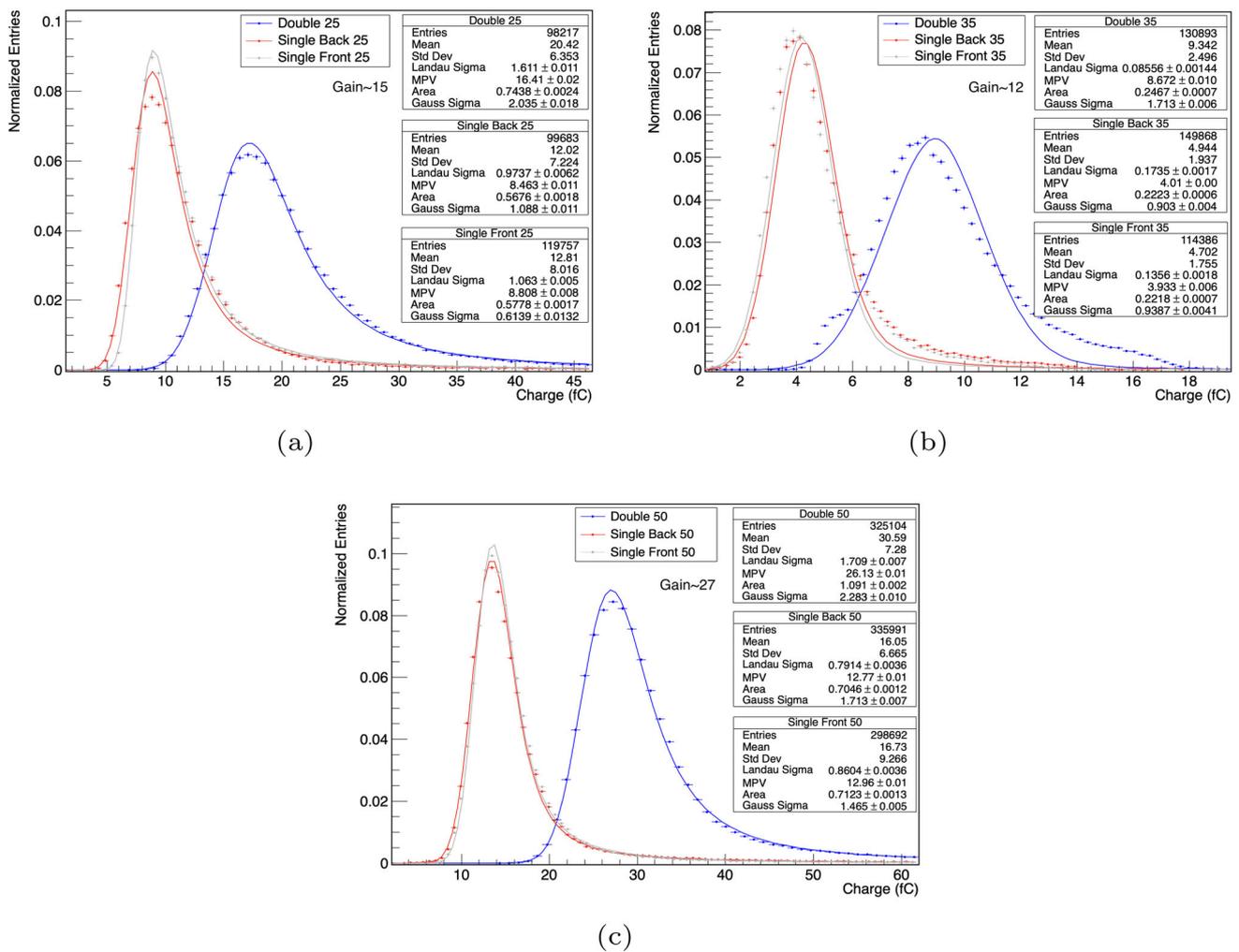


**Fig. 3** Charge distributions for all the DUTs at a gain of 15, 12 and 27 for the FBK25 (a), FBK35 (b) and HPK50 (c) couples, respectively. The distributions are fitted with a convolution of a Gaussian function and a Landau function

For all the measurements reported in this paper, the double LGAD has always been compared with the performances of the single LGAD composing the d-LGAD under test.<sup>5</sup> Therefore, every LGAD thickness will always have three different measurements: two coming from each of the LGAD composing the d-LGAD and one from the d-LGAD itself.

The root mean square (RMS) of the noise (see [3] for more details) and the signal-to-noise ratio (S/N) have been evaluated for each sensor and voltage. In Fig. 2, they are reported as a function of the applied voltage. As can be seen, the noise between single and double sensors is compatible for all thicknesses. The S/N instead is always higher for the d-LGAD, giving already some insight into the better performances reported later in the paper.

### 4 Results

The data analysis was performed following similar procedures to those reported in [3, 10]. In particular, thanks to the oscilloscope readout, the full signal waveforms were recorded and analysed. It was then possible to use the constant fraction discriminator (CFD) method to extract the detector under test (DUT) time resolutions. Moreover, to filter out the high-frequency noise, a smoothing of the LGAD signal was applied with a four-point moving average.

To extract the time resolution of a single DUT (single or double LGAD), a system with three sensors and three differences between the arrival time of each pair of detectors has been considered. The sigma extracted from the fit has then been used to obtain the final time resolution of the three LGADs at a given voltage and CFD.

<sup>5</sup> First, we tested always the d-LGAD. Then, we un-bonded the bottom LGAD in order to test the top one. Lastly, we un-bonded the top LGAD, bonding and testing the bottom one.

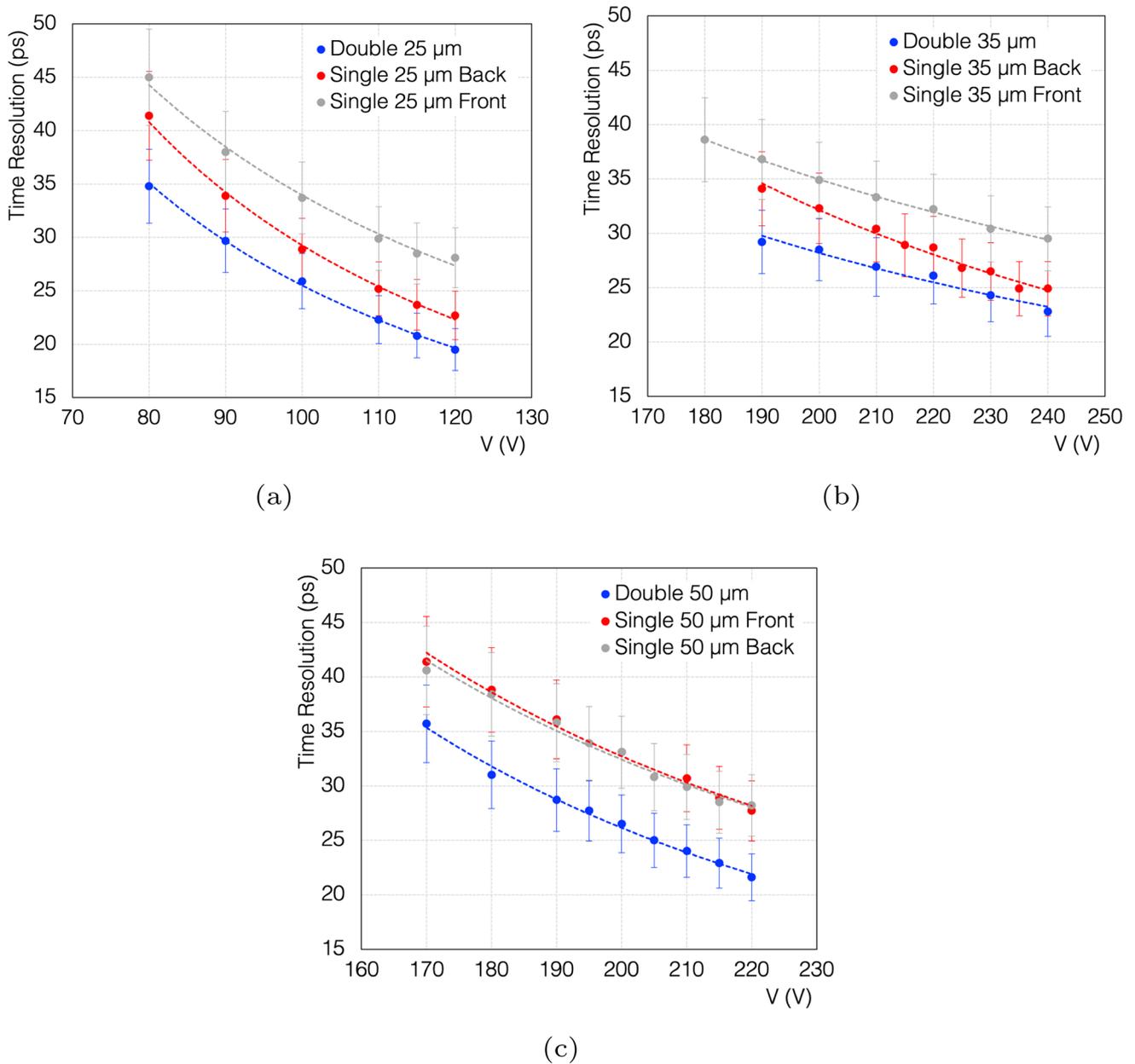
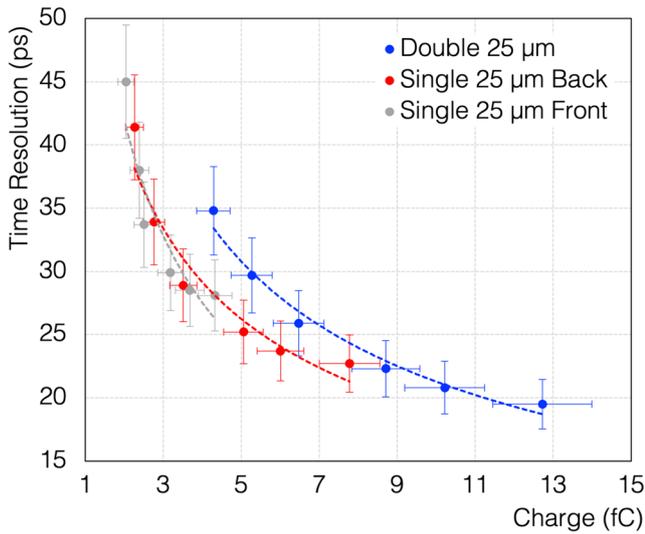


**Fig. 4** Measured time resolution results from the beam test as a function of the voltage applied for all the LGADs tested 25 (a), 35 (b) and 50 (c)  $\mu\text{m}$  for a CFD of 50%, 30% and 30%, respectively. The errors for the measured time resolution have been estimated as 10% of the value. The lines are included to guide the eye

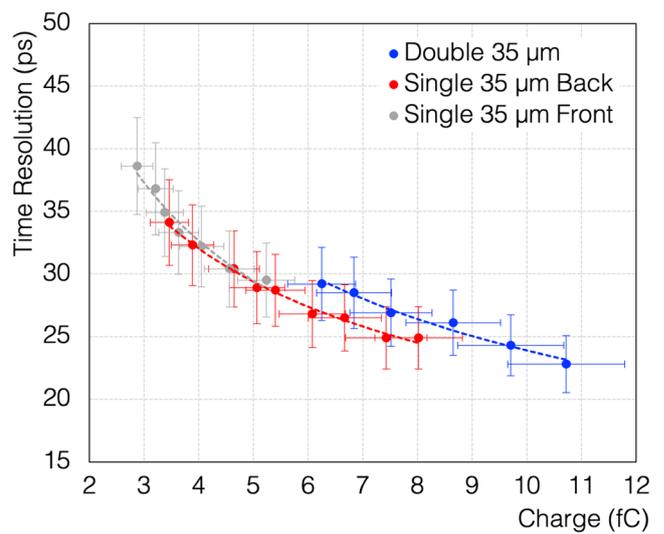
In Fig. 3, the measured charge distributions are shown. Notice that the comparisons between single and the double LGADs have been made at a fixed gain. As can be observed, the d-LGAD always showed a most probable value (MPV) of charge which was double that of the single one, as naively expected, demonstrating the success of a so-built detector and, as a consequence, the potentially less demanding electronic front end that can be realized, thanks to the larger charge in input.

In Figs. 4 and 5, the measured time resolution for a fixed CFD (more details in [3, 10]) is always considered. In Fig. 4, the time resolution as a function of the applied voltage is reported.

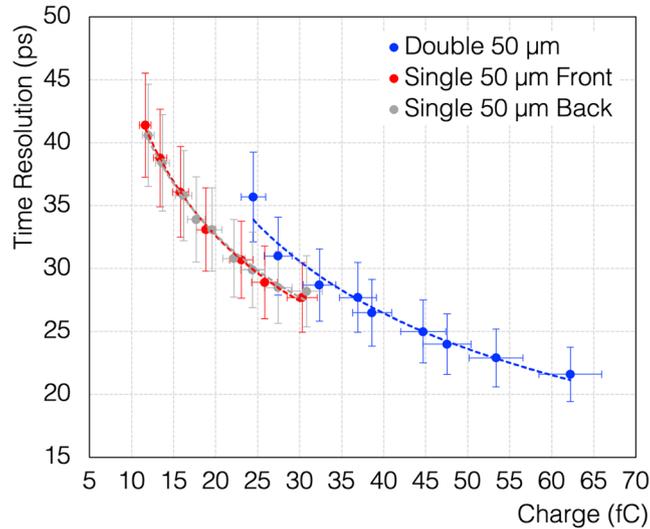
First of all, if compared with [3], the results for all thicknesses are compatible. It can be noticed that the resolutions of the single LGADs are very nicely uniform only for the 50  $\mu\text{m}$  couple, owing to the more uniform sensor wafer (and specifically to the more similar gains for the two sensors). Nevertheless, for all three thicknesses, for a fixed voltage an improvement in the time resolution has been observed with the d-LGADs. A final time resolution of  $\sim 20$  ps has been obtained for all three thicknesses. For the future, new 25 and 35  $\mu\text{m}$  production with increased uniformity could potentially improve the time resolution of d-LGAD, bringing time resolution below 20 ps.



(a)



(b)



(c)

**Fig. 5** Measured time resolution results from the beam test as a function of the charge collected for all the LGADs tested, 25 (a), 35 (b) and 50 (c)  $\mu\text{m}$  for a CFD of 50%, 30% and 30%, respectively. The errors for the measured time resolution have been estimated as 10% of the value. The lines are included to guide the eye

In Fig. 5, the time resolution as a function of the charge is then reported. The plot would be totally similar if plotted vs gain. As expected, the d-LGADs show higher charge with respect to single LGADs at the input of electronics, in particular for uniform wafers and couples, as in the case of the 50  $\mu\text{m}$  thickness.

In Table 2, the best time resolutions reached for the three detectors tested are summarized.

### 5 Conclusions

The study presented in this paper describes a new concept for improving time resolution by coupling two LGADs connected to the same amplifier. All the results have been obtained using a 10 GeV/c beam at CERN-PS. For three different thicknesses of sensors, the performance of the d-LGAD has been compared with that of the single LGADs composing it. The d-LGAD concept shows clear advantages over the standard single LGAD, resulting in better time resolution with the added benefit of a higher charge provided at the

**Table 2** Time resolution for 25, 35 and 50 for a given voltage (or gain) obtained in a beam test set-up at room temperature

	Voltage applied (V)	Gain	Time resolution
FBK25 front	120	24 ± 2	(23 ± 2) ps
FBK25 back	120	43 ± 4	(28 ± 3) ps
d-FBK25	120	35 ± 4	(20 ± 2) ps
FBK35 front	240	17 ± 2	(30 ± 3) ps
FBK35 back	240	27 ± 3	(25 ± 2) ps
d-FBK35	240	15 ± 2	(23 ± 2) ps
HPK50 front	220	63 ± 6	(28 ± 3) ps
HPK50 back	220	64 ± 6	(28 ± 3) ps
d-HPK50	220	59 ± 6	(22 ± 2) ps

input of the amplifier. In particular, the results demonstrate a consistent improvement in time resolution for the d-LGAD compared to the single LGADs, reaching a time resolution of  $\sim 20$  ps for all three thicknesses. Additionally, for all the couples, the charge MPV generated by the d-LGAD is doubled compared to both single sensors, as expected, resulting in a clear advantage for the electronics. At the moment, this stands only as a proof of concept; however, the logical progression would involve a more straightforward integration of this concept, either within the electronics board or directly within the detector itself, potentially utilizing techniques such as through-silicon via (TSV). Overall, this concept presents a promising development for LGAD's performance and paves the way for future implementation of such sensors.

**Acknowledgements** We acknowledge the following funding agencies and collaborations: INFN–FBK agreement on sensor production; Dipartimenti di Eccellenza, University of Torino (ex L. 232/2016, art. 1, cc. 314, 337); Ministero della Ricerca, Italia, PRIN 2017, Grant 2017L2XKTJ - 4DinSiDe; Ministero della Ricerca, Italia, FARE, Grant R165xr8frt\_fare. We wish also to thank the support of the mechanical and electronic workshops of the INFN Unit of Bologna and the CERN-PS operator team for the support. We would also like to thank the CERN Bondlab for their availability during the beam tests.

**Funding** Open access funding provided by CERN (European Organization for Nuclear Research). The study was funded by: INFN - FBK agreement on sensor production; Dipartimenti di Eccellenza, Univ. of Torino (ex L. 232/2016, art. 1, cc. 314, 337); Ministero della Ricerca, Italia, PRIN 2017, Grant 2017L2XKTJ - 4DinSiDe; Ministero della Ricerca, Italia, FARE, Grant R165xr8frt\_fare. The authors received research support from institutes as specified in the author list beneath the title.

**Data Availability Statement** This manuscript has associated data in a data repository. [Authors' comment: The datasets generated during and/or analysed during the current study are available from the corresponding author on reasonable request.]

**Open Access** This article is licensed under a Creative Commons Attribution 4.0 International License, which permits use, sharing, adaptation, distribution and reproduction in any medium or format, as long as you give appropriate credit to the original author(s) and the source, provide a link to the Creative Commons licence, and indicate if changes were made. The images or other third party material in this article are included in the article's Creative Commons licence, unless indicated otherwise in a credit line to the material. If material is not included in the article's Creative Commons licence and your intended use is not permitted by statutory regulation or exceeds the permitted use, you will need to obtain permission directly from the copyright holder. To view a copy of this licence, visit <http://creativecommons.org/licenses/by/4.0/>.

## References

1. G. Pellegrini et al., Technology developments and first measurements of low gain avalanche detectors (LGAD) for high energy physics applications. *NIMA* **765**, 12–16 (2014). <https://doi.org/10.1016/j.nima.2014.06.008>
2. H.F.-W. Sadrozinski et al., 4D tracking with ultra-fast silicon detectors. *Rep. Prog. Phys.* **81**(2), 026101 (2017). <https://doi.org/10.1088/1361-6633/aa94d3>
3. F. Carnesecchi et al., Beam test results of 25  $\mu\text{m}$  and 35  $\mu\text{m}$  thick FBK ultra fast silicon detectors. *Eur. Phys. J. Plus* (2023). <https://doi.org/10.1140/epjp/s13360-022-03619-1>
4. ATLAS collaboration, Technical proposal: A high-granularity timing detector for the ATLAS phase-II upgrade. Technical report, CERN, Geneva (2018). <https://doi.org/10.17181/CERN.CIUJ.KS4H>. <https://cds.cern.ch/record/2623663>
5. C. Cms, A MIP timing detector for the CMS phase-2 upgrade. Technical report, CERN, Geneva (Mar 2019). <https://cds.cern.ch/record/2667167>
6. ALICE Collaboration, Letter of intent for ALICE 3: A next generation heavy-ion experiment at the LHC. Technical report, CERN, Geneva (2022). <https://cds.cern.ch/record/2803563>
7. E. Cerron Zeballos et al., A new type of resistive plate chamber: the multigap RPC. *NIMA* **374**, 132–136 (1996). [https://doi.org/10.1016/0168-9002\(96\)00158-1](https://doi.org/10.1016/0168-9002(96)00158-1)
8. W. Riegler et al., Detector physics and simulation of resistive plate chambers. *NIMA* **500**(1), 144–162 (2003). [https://doi.org/10.1016/S0168-9002\(03\)00337-1](https://doi.org/10.1016/S0168-9002(03)00337-1)
9. V. Sola et al., First results from thin silicon sensors for extreme fluences, in *37th RD50 Workshop Zagreb Online* (2020)
10. F. Carnesecchi et al., Development of ultra fast silicon detector for 4D tracking. *NIMA* **936**, 608–611 (2019). <https://doi.org/10.1016/j.nima.2018.09.110>